# Introducing A Revolution In Theoretical Quantum Computing

## " Generalized Quantum Tunneling Effect and Ultimate Equations for Switching Time and Cell to Cell Power Dissipation Approximation in QCA Devices "

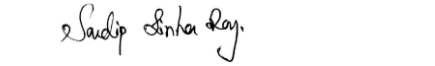

25.12.2017

Soudip Sinha Roy

Project name:
**QCAcalculations**

# About Author



***Soudip Sinha Roy,*** **received the B.Tech degree in Electronics and Communication Engineering from University of Engineering and Management, Jaipur in 2017. He has over four years of research experience in nanoelectronics. His research spaces are nanoelectronics, quantum physics, 2D nanomaterials, astrophysics, quantum gravity. Currently he is the active student member of IEEE, IEEE electron devices society, IEEE Nanotechnology Council and VLSI, IEEE Computer Society Technical Committee, IEEE Council on Electronic Design Automation. He is the reviewer of two peer reviewed nanoscience journals.**

**Email id** *Main email:* soudipsinharoy@gmail.com
*Other email:* soudipsinharoy@physicist.net

Website: www.thessr-library.cf/
DOI: 10.13140/RG.2.2.23039.71849
Date of publication: 25th December 2017

**Cite this article (reference style):**

**S. S. Roy, "Generalized Quantum Tunneling Effect and Ultimate Equations for Switching Time and Cell to Cell Power Dissipation Approximation in QCA Devices", doi: 10.13140/RG.2.2.23039.71849, (self-publication).**

Author's signature

Self-Publishing

# Generalized Quantum Tunneling Effect and Ultimate Equations for Switching Time and Cell to Cell Power Dissipation Approximation in QCA Devices







***Nowadays quantum-dot cellular automata has been playing a major challenge in competition of developing molecular circuits which overcomes certain fatal complications of CMOS devices for instance impurity inconsistency, high device latency etc. Quantum-dot cellular automata empires the quantum binary logic gate designing technology by the help of fastest quantum bits. The electronic orientation assigns the binary q-bits inside the q-cells. In this letter one novel methodology for tunneling barrier resistivity analysis and device latency calculation have proposed. The tunneling barrier resistivity has propounded with a generalized mathematical expression to reveal the instantaneous effect of barrier resistance to the electron during tunneling. Proposed technique for switching time computation explores the signal propagation delay by considering the directional flow of quantum signals through different cells under different clock zones. Furthermore, in this letter one novel cell wise energy and power dissipation computation technique has proposed which offers a very accurate power drop data for the QCA wires. The proposed mathematical expressions are flexible enough for computing the power drop for any homoaxial wire and for any off centered or heteroaxial wire. This contribution extends a previous work on switching time, provided in reference.***

▪ **Relevant Keys—Quantum computing -- tunneling equations -- switching time -- device latency -- power dissipation.**

## I. INTRODUCTION

Quantum-dot cellular automata introduces the quantum logic gates with a controllable electron tunneling facility for the purpose of reconfiguring the electronic positions to attain the lightning device speed. The binary logic states are defined by the electron configuration change. The right handed electronic configuration terms the high logic state '1' and the left handed configuration states the lower logic state '0', *fig.* ***1a*** ***[1]-[5]***. *fig.* ***1b*** shows the QCA three input majority logic system, fig. ***1c*** is a clocked binary wire and the fig. ***1d*** is 7 cells inverter layout.

In this contribution the tunneling barrier resistivity has mathematically calculated and formulized into a mathematical form which is able to compute the instantaneous behavior of the electrons during tunneling ***[6]-[10]***. Furthermore, the signal propagation delay computation methodology has proposed which explores the delay of the signals in propagation from one cell to another. In this letter a novel power drop computation methodology has proposed which is able to monitor the power dissipation of each cell of a binary wire weather it is homoaxial or heteroaxial. This paper is an extended version of a previous publication on QCA device cell wise switching time approximation ***[2]***.

Sudip Sinha Ray

Author's signature

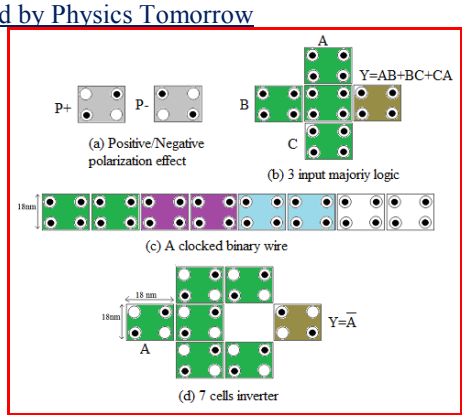


**Fig. 1** (a) Positive/Negative polarization effect, (b) 3 input Majority gate, (c) A clocked binary wire, (d) 7 cells inverter

## II. Aquired Contents From Previous Paper

Layout of 2 bit binary to gray code converter. This is a 2 bit code converter has designed followed by the layered design concept. Each atomic layer has separated by 11.50 nm from another. In this layout three layers have used for avoiding the wire crossover complications *[2], [11]-[21]*.

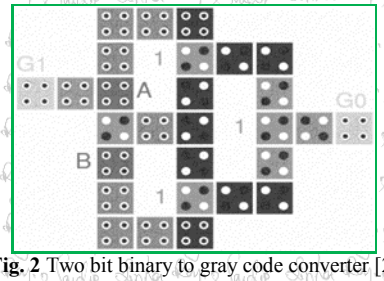


**Fig. 2** Two bit binary to gray code converter [2]

This is the equation which states the tunneling rate in terms of frequency. The tunneling rate equation is given by **[2]**,

$$\Gamma=\frac{1}{\varepsilon_r\varepsilon_0 e R_T}\left((1-e^{\frac{E_{ij}}{KT}})\right)^{-1}\ \text{Hz} \qquad \textbf{(1)}$$

This is ***S-instantaneous tunneling density*** **(SITD)**, which defines the tunneling density at every instant inside the tunneling isolation barrier,

$$\hbar\upsilon=\frac{d\Gamma}{dE_B}=\left|\frac{1}{\varepsilon_r\varepsilon_0 eKTR_T}\cdot\frac{1}{e^{\frac{E_{ij}}{KT}}(1-e^{\frac{-E_{ij}}{KT}})^2}\right| \qquad J^{-1}sec^{-1}$$

## III. Analysis Of Tunneling Phenomena And Barrier Resistivity Calculation

### A. *Calculation of barrier resistivity through tunneling rate and effective tunneling distance*

Below fig. 3 is the model of the tunneling barrier where V stands for barrier potential (in height) and r is the barrier thickness.

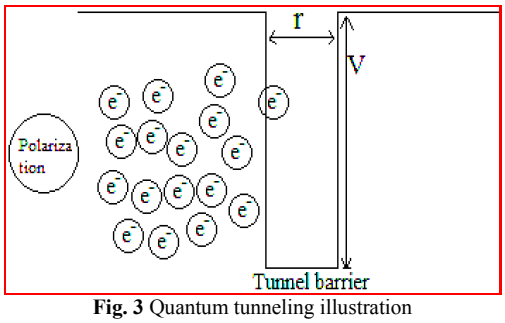


**Fig. 3** Quantum tunneling illustration

The **eq. 1** provides the numerical identification of the tunneling rate ***[2],*** which is inversely proportional to the tunneling resistance $R_T$. The value of $R_T$ is dependent on the thickness of tunnel barrier 'r' and the potential height of the barrier 'V', fig. 3. The resistivity of this barrier is assumed as $\rho_T$, therefore the $R_T=\frac{\rho_T*V}{r*V}=\frac{\rho_T}{r}$. By replacing this value of $R_T$ in **eq. 1**, it is formularized as,

$$\Gamma=\frac{1}{\varepsilon_r\varepsilon_0 e R_T(1-e^{\frac{E_{ij}}{KT}})}=\frac{r}{\varepsilon_r\varepsilon_0 e\rho_T}\left(1-e^{\frac{E_{ij}}{KT}}\right)^{-1} \qquad \textbf{(2)}$$

If $\frac{1}{\varepsilon_r\varepsilon_0 e}$ is assumed as a constant value then the tunneling rate is dependent only on the variation of the 'r', '$\rho_T$' and $\left(1-e^{\frac{E_{ij}}{KT}}\right)^{-1}$. Therefore, this is mathematically expressed as,

$\Gamma\propto\frac{r}{\rho_T}\left(1-e^{\frac{E_{ij}}{KT}}\right)^{-1}$ which defines the proportionality.

The width of the tunnel barrier is relative in nature. After starting the tunneling the effective value of **r** starts to decrease likewise r, r-$\Delta$r, r-2$\Delta$r, r-3$\Delta$r and so on, fig. ***3***. Along with the decrement of **r** the effective resistivity gradually reduces. Therefore, there are two different parts of **eq. 2**, one is a constant part and the second one is a variable part.

$$\Gamma=\frac{r}{\varepsilon_r\varepsilon_0 e\rho_T}\left(1-e^{\frac{E_{ij}}{KT}}\right)^{-1}$$

$$\Gamma=\frac{r}{\varepsilon e\rho_T}\left(1-e^{\frac{E_{ij}}{KT}}\right)^{-1} \qquad \textbf{(3)}$$

$$\Gamma=\Gamma_0\left(1-e^{\frac{E_{ij}}{KT}}\right)^{-1}$$

$\Gamma_0$ is named as ***S-factor*** which is equals to $\frac{r}{\varepsilon e\rho_T}$.

This equation is re-expressed as where d is the effective tunneling distance ***[2],***

$$\Gamma=\Gamma_0\left(\frac{c}{\Gamma d}\right)^{-1}$$

$$d^{-1}=\Gamma_0 c^{-1}$$

$$d=\Gamma_0^{-1}c$$

After replacing by the $\Gamma_0$ the equation becomes, $d=\frac{\varepsilon e c\rho_T}{r}$

Sudip Sinha Ray

Author's signature

Therefore, the tunneling barrier resistivity is defined as,

$\rho_T = \frac{d\,r}{\varepsilon e c}$

*B.* ***Solution for tunneling barrier resistivity*** $\rho_T$

Equation 3 is the simplified form of tunneling rate Γ. Let assume the barrier thickness is **x** nm. Hence, the effective tunneling path for the electron is x nm. The electron starts its journey from 0 nm and it finishes the journey at x nm, fig.***3***. After integrating the **eq. 3** in both sides with **dx** the resulting equation provides the speed of tunneling. The calculated tunneling speed of the electron is mathematically expressed as,

$v = \frac{r*x}{\varepsilon e \rho_T}\left(1 - e^{\frac{E_{ij}}{KT}}\right)^{-1}$

The quantum tunneling occurs at the speed of light. Therefore, in above equation, v=c= $3\times 10^8$ m/sec. After replacing the value of v from above equation now it is rearranged as,

$\rho_T = \frac{r*x}{\varepsilon e c}\left(1 - e^{\frac{E_{ij}}{KT}}\right)^{-1}$

Practically the value of **r** is equals to **x** as fig. ***3***, therefore, this equation is further extended as,

$\rho_T = \left|\frac{r^2}{\varepsilon e c}\left(1 - e^{\frac{E_{ij}}{KT}}\right)^{-1}\right|$

In purpose of point to point investigation of tunneling barrier resistivity r can be written as (r-nΔr), where the effective value of the **r** is undertaken only. **Δr** is the small increment in effective tunneling distance. Assuming that Δr is a uniform increment. Moreover, n is the integer number which defines the current state (current position of electron inside tunnel barrier) of tunneling. It gives the values like 0, 1, 2, 3⋯. If the electron is its initial state (before tunneling) then the n=0, if next to initial state inside the tunneling barrier then n=1 and so on. Therefore,

$\rho_T = \left|\frac{(r-n\Delta r)^2}{\varepsilon e c}\left(1 - e^{\frac{E_{ij}}{KT}}\right)^{-1}\right|$

From paper ***[2]*** the value of $\left(1 - e^{\frac{E_{ij}}{KT}}\right)^{-1}$ is found as, $\frac{c}{\Gamma d}$

$\rho_T = \left|\frac{(r-n\Delta r)^2 \Gamma d}{\varepsilon e c^2}\right|$ **(4)**

**Equation 4** is the generalized form of tunneling barrier resistivity. This **eq. 4** is named as ***S-tunneling resistivity***.

**CASE 1:** When n=0;

$\rho_{T\,MAX} = \left|\frac{(r)^2 \Gamma d}{\varepsilon e c^2}\right| = \left|\frac{d^3 \Gamma}{\varepsilon e c^2}\right|$ Ω m

At this situation the electron faces the maximum resistivity from the tunnel barrier.

**CASE 2:** When the electron is absolutely at the center of the tunneling barrier then the condition is written as, $n\Delta r = \frac{r}{2}$.

$\rho_{T\,MID} = \left|\frac{(r)^2 \Gamma d}{4\varepsilon e c^2}\right| = \left|\frac{d^3 \Gamma}{4\varepsilon e c^2}\right| = \frac{\rho_{T\,MAX}}{4}$ Ω.m

Therefore, at the middle of the barrier the resistivity is four times lesser than the initial resistivity.

**CASE 3:** After the electron reaches to another dangling bond it is mathematically expressed as, nΔr=r.

$\rho_{T\,REST} = 0$ Ω.m

Tunneling barrier resistance $R_T$ is defined as, $\frac{\rho_T \times V}{A}$; Here A is the effective area which is defined by r×V, as fig. ***3***.

Therefore, $R_T = \frac{\rho_T}{r}$; ***r*** defines the effective tunneling distance which is equals to ***d***. This **d** is the width of the tunnel barrier. The tunneling occurs at speed of light. So, **r** is the product of **c** and **t**. Therefore this tunneling resistance is redefined as, $R_T = \frac{\rho_T}{ct}$; ***c*** is the speed of light and ***t*** is the time taken by the electron to penetrate the barrier completely. By putting the value of $\rho_{T\,MAX}$ in $R_T$ equation, the maximum value of $R_T$ is expressed as,

$R_{T_{Max}} = \frac{\rho_{T\,Max}}{ct} = \frac{t^2 \Gamma}{\varepsilon e}$

Similarly, the intermediate tunneling barrier resistance is expressed as,

$R_{T_{MID}} = \frac{t^2 \Gamma}{4\varepsilon e}$

Now, the value tunneling resistance $R_{T_{Max}}$ is put in **eq. 1**,

$\Gamma = \frac{\varepsilon e}{\varepsilon e t^2 \Gamma}\left(1 - e^{\frac{E_{ij}}{KT}}\right)^{-1}$

$\Gamma = \frac{1}{t}\left(1 - e^{\frac{E_{ij}}{KT}}\right)^{-1/2}$

In a situation if in case, $E_{ij}$ =0 then only the inverse of switching time will be the tunneling rate as following expression,

$\Gamma = \frac{1}{t}$

From the calculations of section IV, the tunneling time $t_1$ is equals to the **t** in above equation. Therefore, the above tunneling rate equation is reformulated as,

$\Gamma = 5 \times 10^{16}\left(1 - e^{\frac{E_{ij}}{KT}}\right)^{-1/2}$ Hz

For QCA devices $50 \times 10^{15}$ Hz is a constant value which is named ***S-frequency***. That is the QCA device operating frequency, from **section IV**.

After a hard calculation the SITD has redefined as,

$h\upsilon = \frac{1.09\times 10^{36} e^{\frac{E_{ij}}{2KT}}}{T - Te^{\frac{E_{ij}}{4KT}}}\ J^{-1} sec^{-1}$

Sadip Sinha Ray

Author's signature

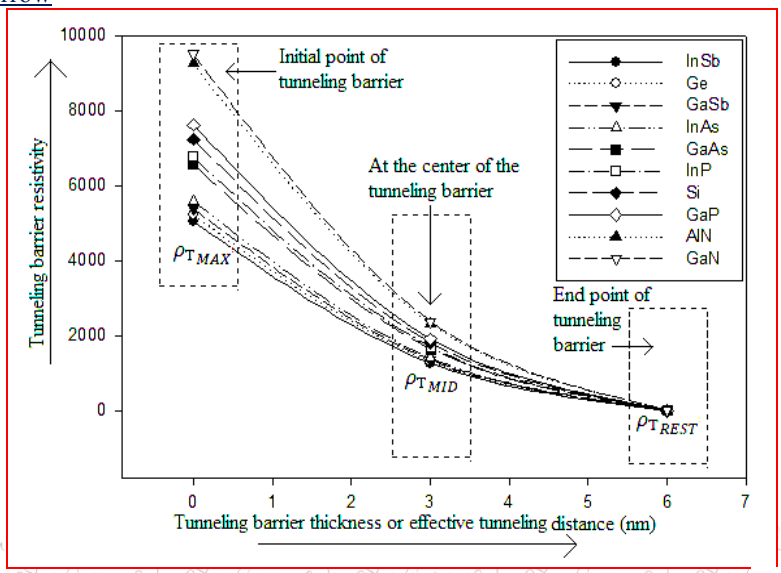


**Fig. 4** Tunneling barrier resistivity analysis for several semiconductors by the help of above case studied equations. The $\rho_{T_{MAX}}$, $\rho_{T_{MID}}$ and $\rho_{T_{REST}}$ are briefly illustrated in above graph (according to case 1, case 2 and case 3 equations of barrier resistivity)

This theory imparts, the Silicon has a barrier resistivity $\rho_{T\,MAX}$ = 7.373624 $\times 10^5$ Ω cm. In standard, the resistivity of an intrinsic Si at 300K is 3.5 $\times 10^5$ Ω cm. This calculation proves that the resistivity becomes approximately double when the bulk material changes to respective the nanomaterial. Typically the resistivity increases when the temperature decreases as a result of decrease of the random lattice phonon. QCA devices can operate at maximum 17K temperature that avoids the electron ejection form the DB. Thereby, the resistivity increment is theoretically proven as a highly logical phenomena.

## IV. Scaling Of QCA Cells In Nanoscale

In precise atomic view the Q-cells contain four q-dots which are typically formed by the dangling bond creation on the atoms are present in the lattice surface. In practice the removal of four hydrogen (H) atoms from four silicon (Si) atoms in (100) Hydrogen doped Si quantum dot results this dangling bond (DB) which are suitable for localizing the electrons ***[3], fig. 5, 6***. Usually q-dots can have maximum 8 nm to 9 nm diameter which are capable to localize 10 to 15 atoms in it. But each Si atom can perform as a distinct quantum dot, this is the most versatile property of **Si** qdots, just because of that Si is highly preferable for QCA device fabrication purpose. But in QCA technology the q-dots have 5 nm diameter ***[3], [20],*** that is the assembly of a very few Si atoms approx. 2 to 4.

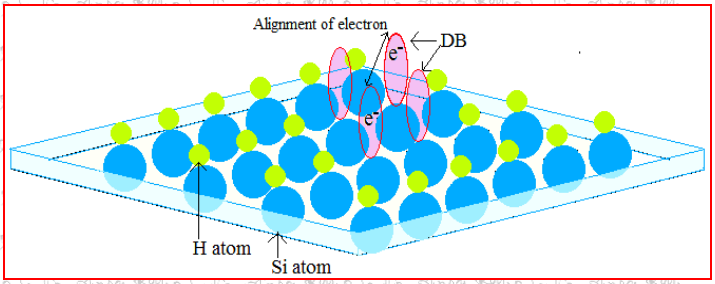


**Fig. 5** Effect in DB under P+ (positive) polarization

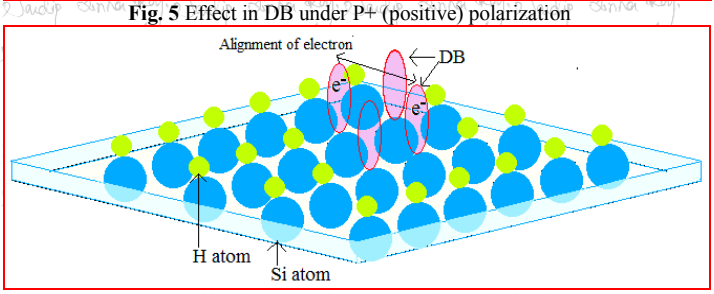


**Fig. 6** Effect in DB under P- (negative) polarization

Under the effect of positive or negative polarizations the alignment of the electrons are shown in atomic view, ***fig. 5, 6***. The blue circles represent the silicon (**Si**) atoms and the greens are hydrogen (**H**) atoms inside a quantum cell. Each corner of this cell has one quantum dot. Therefore, every cell contains four quantum dots. In the second row of this lattice two hydrogen atoms have removed from the 4th and 5th silicon atoms and similarly in the third row of this the lattice from 3rd and 4th silicon atoms two hydrogen atoms have removed, ***fig. 5, 6***. Due to the removal of 4 H atoms the four dangling bonds have created. The DBs are the unsaturated valance which are capable to localize the electrons. Using Scanning Tunneling Microscopy (**STM**) the precise electron implantation is

Sadip Sinha Ray

Author's signature

possible inside the DB. Those implanted electrons become free but immobile in natural condition (depolarized state). When the external polarization (in terms of electric field) is applied then the electrons gain sufficient energy for being tunnelable through tunneling barrier.



***Dimensional scaling of quantum cells***

One q-cell has $18 \times 18$ $nm^2$ area, ***fig.7.*** Therefore, the length and the breadth both are equals to 18 nm. Out of 18 nm, (5+5) 10 nm space has covered by two upper q-dots. Remaining 8 nm space has a distribution like (1+6+1) nm. Each q-dot has the 1 nm separation from the end point (grain boundary), ***fig, 7.*** Therefore, the effective space between two q-dots are equals to 6 nm.

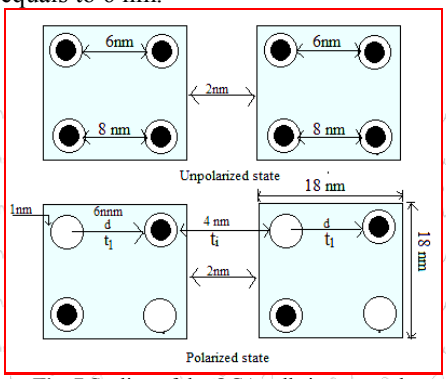


**Fig. 7** Scaling of the QCA cells in nanoscale

The separation between two q-cells are 2 nm. Hence, the effective intermediate spacing between two q-dots of two different q-cells are given by 4 nm, ***fig. 7 [21].***

The quantum tunneling occurs at the speed of light i.e. 300, 000, 000 m/sec. Therefore, the tunneling time is calculated as $t_1 = \left({}^{6 \times 10^{-9}}/_{3 \times 10^8}\right) \cong 2 \times 10^{-2}$ attosecond.

The quantum signal propagation has the lightning speed during travelling from one cell to another cell. Hence, the inter-cell switching time is expressed as, $t_i = \left({}^{4 \times 10^{-9}}/_{3 \times 10^8}\right)$ sec $\cong 1.33 \times 10^{-2}$ attosecond.

The net switching time for two cells is formularized as,

$t_s = 2t_1 + t_i$

$= 5.33 \times 10^{-2}$ attosecond.

$\Gamma = \frac{1}{t_1} = 50$ Peta Hz which is the operating frequency of the four q-dot QCA devices. One QCA cell is capable to be operated at 50 PHz frequency that is significantly higher than CMOS, NMOS and other electron island devices.

## V. Proposed Latency Diagram for Device Latency Computation

In this section the latency of the proposed 2 bit binary to gray code converter has analyzed by the help of proposed latency diagram approach. This latency diagram is calculating the device latency theoretically with the proposed algorithm. In this process the whole circuit is subdivided into a few smaller segments where the signal flow is presented explicitly, fig. 8, 9. The general equation $t_s = (C-1)\Gamma^{-1}$ ***[2]*** for switching time computation have used to approximate the net switching time of this 2 bit binary to gray code converter device. Below diagrams show the calculation procedure of the device latency.

**Proposed algorithm for signal propagation delay (device latency) computation:**

***Begin***

1. *Select the inputs and outputs of the respective circuit.*
2. *Draw the proper signal flow directions on the layout from inputs towards outputs.*
3. *Group the cells based on the clock and their positions.*
4. *Assign the weights of each group based on number of cells present in a group.*
5. *Use this equation* $t_s = (C-1)\Gamma^{-1}$ *and calculate the switching time for each group of cells using the obtained weights i.e. C.*
6. *Perform the simple addition of all the obtained results.*

***End.***

After designing the cell to cell interaction phenomena, the following diagram is achieved which explains the signal flow direction within the q-cells, ***fig. 8***.

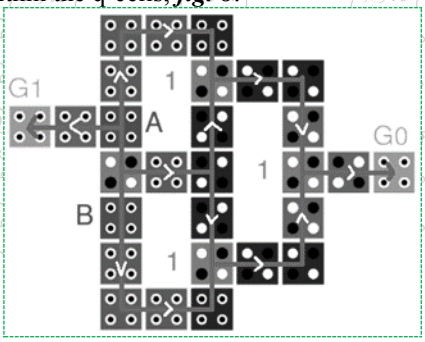


**Fig. 8** Signal flow directions in 2 bit binary to gray code converter

Sadip Sinha Ray

Author's signature

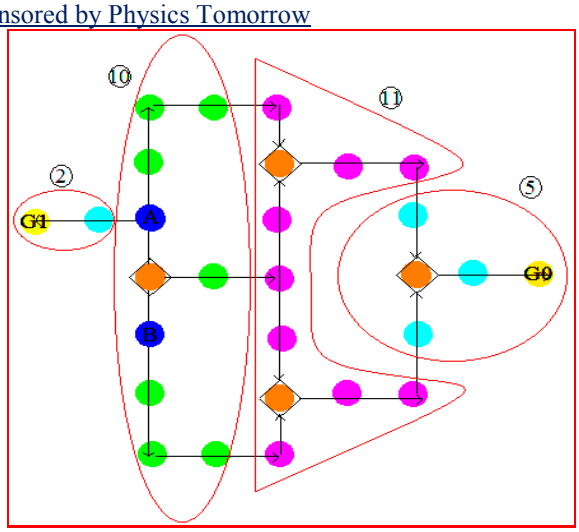


**Fig. 9** Device latency diagram for proposed 2 bit binary to gray code converter

In above diagram ***fig. 9***, the code converter layout has subdivided into several group of cells depending upon the signal flow strategy which have undertaken to approximate the signal propagation latency during the device operation. This diagram has some weighted values which is determined by the number of cells are present in a group as indicated above. The entire mathematical process have illustrated below.

The general equation for switching time is $t_s = |(C-1)\Gamma^{-1}|$ ***[2].*** Therefore, only with the known values of C and $\Gamma$ this equation is solvable. From section IV, the value of $\Gamma$ is 50 Peta Hz. The proposed latency matrix is given as $L=[2\ 7\ 2\ 2\ 6\ 3\ 3\ 3]_{1\times 8}$ which is generated from ***fig. 9***. This matrix elements depend on the weights of this device latency diagram.

**Calculation**

$t_{s\ 2}$= (2-1)× $50^{-1}$ = 0.02 attosecond.
$t_{s\ 10}$= (10-1)× $50^{-1}$ = 0.18 attosecond.
$t_{s\ 11}$= (11-1)× $50^{-1}$ = 0.20 attosecond.
$t_{s\ 5}$= (5-1)× $50^{-1}$ = 0.08 attosecond.

Hence the summed value of all of these provide the device latency or signal propagation delay. The sum of (0.02+0.18+0.20+0.08) is equals to 0.48 attosecond. Therefore, the value of $t_s$ is defined as 0.48 attosecond. It is established that this device has 0.48 attosecond signal propagation delay.

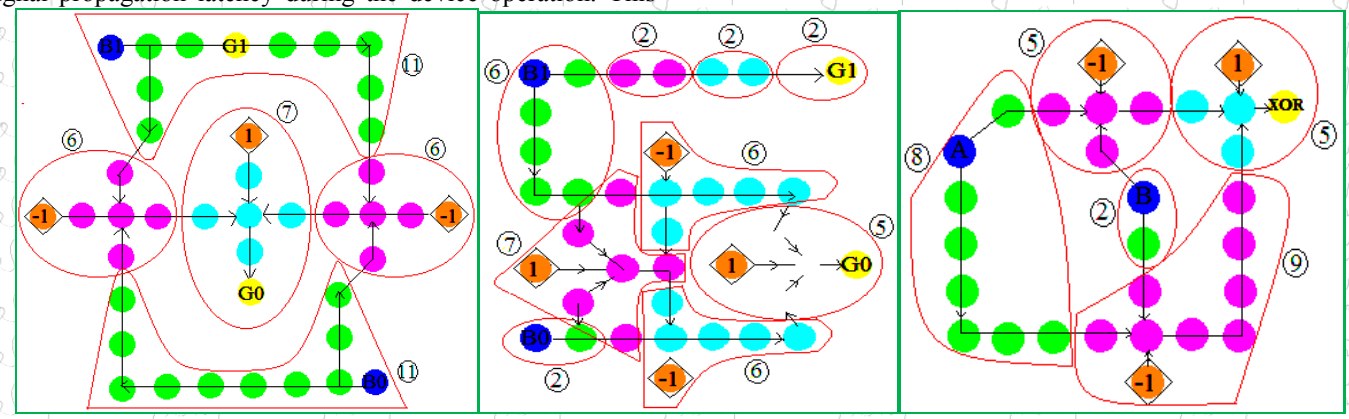


(a) **[9]** (b) **[11]** (c) **[12]**

(d) **[13]**

**Fig. 10** Latency diagrams for erstwhile designs by proposed methodology. **(a) [9], (b) [11], (c) [12], (d) [13]**

Author's signature

In above diagrams the device latency of the erstwhile designs have computed by proposed methodology. Fig. ***10 a,b*** are the 2 bit binary to gray code converter designs and ***fig. 10 c,d*** are the XOR gate designs.

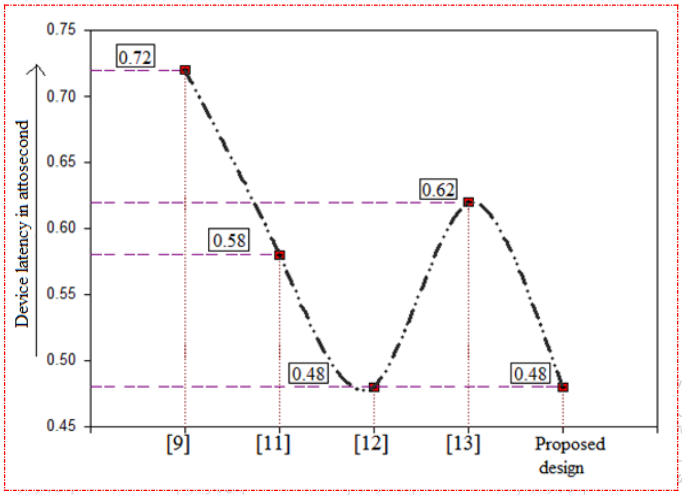


**Fig. 11** Device latency comparisons for previous designs (values from fig. 10 latency diagrams)

## VI. Proposed Energy Dissipation Computation

In QCA devices the energy dissipation is mainly dependent upon two major things, one is displacement between two cells and axial angular displacement between two cells, ***fig. 12***. The kink energy of the cells increases if the liner cell displacement and translation angle $\theta$ increases. This relationship is mathematically expressed as,

$$E_{diss} = E_k f(r) \sin(n\theta)$$

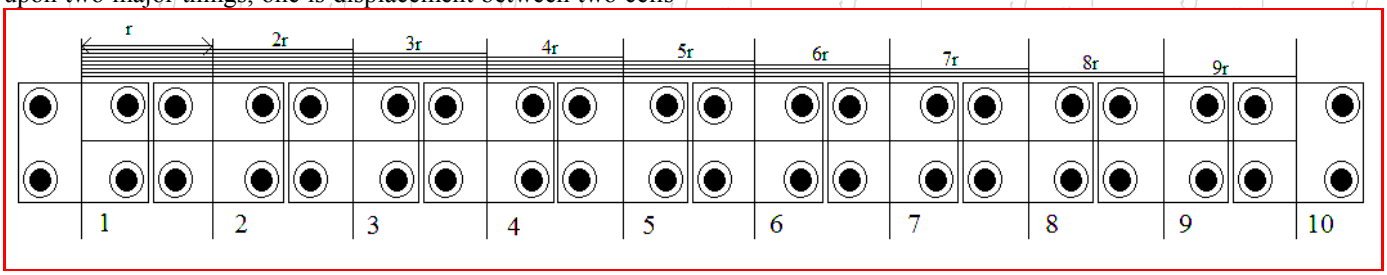


**Fig. 12** Linear scaling of a QCA binary wire

In this case the linear displacements among the cells have been illustrated by sketch. In above figure, **r** is the distance between two cells and gradually **r** increases with the increment of number of cells. Then it is denoted as, $r'$=(C-1)r; where C is the number of cells. From fig. 7, the computed value of **r** is 20 nm.

The saved energy $E_s$ is expressed as,

$E_s = E_T - E_{diss}$

$$E_s = E_T - \frac{r'}{l}\left((C-1) + \frac{\sin(4\theta)}{\sin(8\theta)}\right) E_k \qquad (5)$$

$E_T$ is the total energy that is provided for polarizing the driver cell. The saved energy is the amount energy that will be utilized to latch the next cells.

Dissipate energy is given as,

$$E_{diss} = \frac{r'}{l}\left((C-1) + \frac{\sin(4\theta)}{\sin(8\theta)}\right) E_k \qquad (6)$$

In above equation $l$ is the dimension of a single qcell and $r'$=(C-1)r, is the separation between qcells.

**Case 1:** For a homoaxial binary wire, the value of $\theta$ approaches zero that modifies the above **eq. 5** as,

$$E_s = E_T - \frac{r'}{l}(C-1)E_k$$

In above ***fig.12***, if the cell 5 is selected which saved energy to be calculated then $E_s$ is written as,

$$E_s = E_T - \frac{20}{18}(5-1)E_k$$

$$E_s = E_T - 4.44E_k$$

Sadip Sinha Ray

Author's signature

Correspondingly, this approach is applicable for any cell that is present in any homoaxial binary wire. If any cell is displaced upward or downward then accordingly the value of **r** and $\boldsymbol{\theta}$ changes. Through this mathematical expression the power drop is also become computable.



The dissipated power $P_{diss}$ is given as the ratio of the energy drop and switching time. This ration directly explicates the cell wise power drops.

$$P_{diss} = \frac{E_{diss}}{t_s}$$

For a homoaxial wire, as ***fig. 12***, the power dissipation is expresses by,

$$P_{diss} = \frac{\frac{r'}{l}E_k}{\Gamma^{-1}} = \frac{\Gamma r' E_k}{l}$$

For $18 \times 18nm^2$ dimensional qcell the power dissipation equation is generalized as,

$P_{diss}$=2.78× $10^{23}$ $r'E_k$ W

Assuming a standard value of the kink energy for a cell, $E_k$=3.14× $10^{-8}$ pJ

$P_{diss}$=8722.22$r'$

The above equation is independent to cell count, but it has a factor of distance **(r)** which is a function of number of linearly used cells.

**Case 1:** For the second cell the value of $r'$ is expressed as **r**, as ***fig. 12***.

Then,

$P_{diss}$=8722.22r

=8722.22×20× $10^{-9}$

=1.744 mW

**Case 2:** For the 6th cell value of $r'$ is **5r**, as ***fig. 12***.

$P_{diss}$=5r×8722.22

=8.722 mW

Similarly, by this approach for other cells it is possible to calculate the dissipated power.

Therefore, in case of a homoaxial wire, the power dissipation becomes independent of the number of cells. This only varies with the change in the value of r. If the cell count increases then the logical increment of the value of **r** comes about that is represented by $\boldsymbol{r'}$, in **table I**.

In below figure one off centered QCA cell has shown.

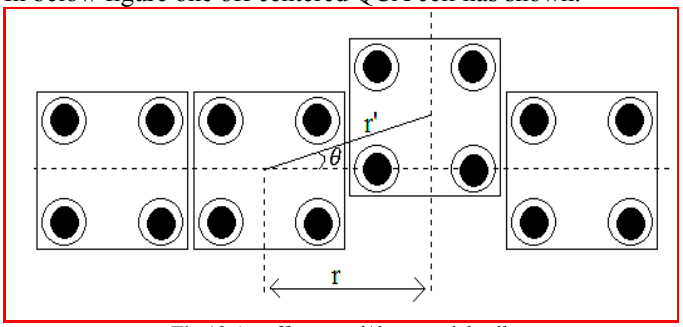


**Fig.13** An off centered/ heteroaxial cell

TABLE I. ENERGY AND POWER DISSIPATION DATA FOR 6TH CELL OF THE QCA WIRE

| Sr. No | Translation angle ($\theta^{\circ}$) | $r'$=5r (nm) | $E_{diss}$ (J) | $P_{diss}$ (mW) |
|---|---|---|---|---|
| **1** | 0 | 20× 5=100 | - | - |
| **2** | 0.1 | 100.5 | 0.9642× $10^{-18}$ | 9.642 |
| **3** | 0.2 | 102.05 | 0.9791× $10^{-18}$ | 9.791 |
| **4** | 0.3 | 104.67 | 1.004× $10^{-18}$ | 10.04 |
| **5** | 0.4 | 108.57 | 1.041× $10^{-18}$ | 10.41 |
| **6** | 0.5 | 113.94 | 1.093× $10^{-18}$ | 10.93 |
| **7** | 0.6 | 121.16 | 1.162× $10^{-18}$ | 11.62 |
| **8** | 0.7 | 130.75 | 1.254× $10^{-18}$ | 12.54 |
| **9** | 0.8 | 143.53 | 1.377× $10^{-18}$ | 13.77 |
| **10** | 0.9 | 160.87 | 1.543× $10^{-18}$ | 15.43 |

Above table interprets the energy and power dissipations of the 6th cell in the QCA wire due to the variation in translation angle ($\boldsymbol{\theta^{\circ}}$), ***fig. 12***. Through this approach the energy dissipation of any particular QCA cell can be achieved and the entire behavior of the wire can be justified mathematically. It is recommended that by keeping the notice on the dissipated energy to the last cell of the wire through this method, the driving energy should be provided to the driver cell. This could provide an idea of the effective power utilization and the power drop through the QCA circuit.

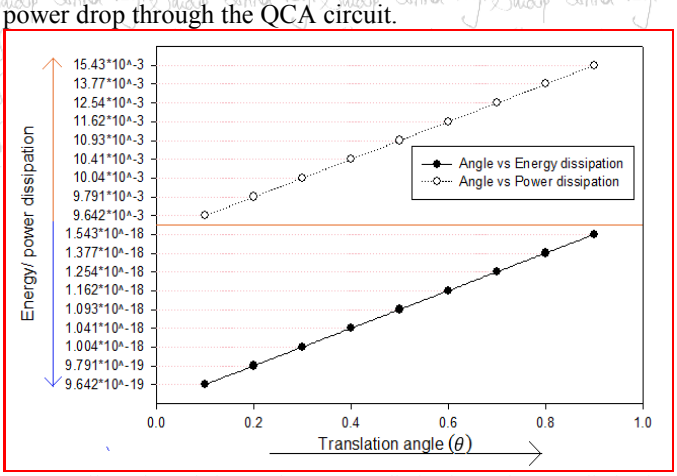


**Fig. 14** Effect of translation angle on power dissipation and energy dissipation of the 6th cell of the QCA binary wire, fig. 12.

TABLE II. PERCENTAGE CHANGE IN POWER DROP FOR THE VARIATION OF TRANSLATION ANGLE

| Sr. No. | Translation angle ($\theta^{\circ}$) | Percentage change (%) |
|---|---|---|

Sudip Sinha Ray

Author's signature

| | | |
|---|---|---|
| **1** | 0 | No change |
| **2** | 0.1 | 10.54 |
| **3** | 0.2 | 12.25 |
| **4** | 0.3 | 15.11 |
| **5** | 0.4 | 19.35 |
| **6** | 0.5 | 25.31 |
| **7** | 0.6 | 33.22 |
| **8** | 0.7 | 43.77 |
| **9** | 0.8 | 57.87 |
| **10** | 0.9 | 76.90 |

Above **table II**, enlightens the change in power dissipation in percentage for the 6th cell if the translation angle variation occurs, remarkably. This analysis justifies the gradual increment of the dissipated energy compared to the homoaxial wire, due to the increment in the translation angle. This section concludes and proves the power dissipation characteristics of a QCA cell in a wire and justifies the deviation in power drop for an off centered cellular wire.

## VII. Conclusion

In present quantum nanotechnology there are many instances alike Carbon Nanotube FET (CNTFET), SpinFET, Single electron transistors (SET), Electron Spin Devices etc. which are highly adaptive in performance. Quantum-dot Cellular Automata is also a molecular logic synthesis technique which is fastest in performance than others. The quantum tunneling effect gives it the lightning speed of operation. In this research letter two major things of QCA devices have analyzed. One is the tunneling barrier resistivity and another one is the switching time. It is mathematically proved that the variation of the barrier resistivity causes the variation in electron tunneling probability which affects the tunneling rate notably. The proposed ***S-tunneling resistivity*** equation is enough to explain the instantaneous behavior of the tunnel barrier during tunneling. The novel switching time commutation technique provides a major sense in QCA devices by calculating the switching time accurately.

In section III, the tunneling barrier resistivity equation has proposed which reveals the nature of electron tunneling during the penetration of the electron through the barrier. In the next context the switching time computation procedure has proposed through a mathematical model which explicates the signal propagation delay along the Q-cells. This signal propagation time is mathematically indicated by $t_s$ which is approximated by several complex calculations in **section IV and V**. Proposed theory imparts the operating frequency of the device is **50 Peta Hz** and the time required for an electron to tunnel the barrier is $2 \times 10^{-2}$ **attosecond**. By the help of proposed latency computation methodology the device latency of 2 bit binary to gray code converter has solved and the latencies for previous designs explored from erstwhile articles have also illustrated in section V. This article contributes more by presenting a novel energy and power dissipation analysis methodology. In section VI, the dissipated power equation has proposed that able to calculate the change in power drop due to the angle variation in case of off centered cell. It is reported that if $0.1^{\circ}$ angular translation occurs then the power drop rises to **10.54%** and so on for the further angle increment.

## References

[1] ITRS: International Technology Roadmap for Semiconductors (ITRS), website (2011). http://www.itrs.net/

[2] Soudip Sinha Roy, "Towards the approximation of cell wise switching time in Quantum-dot Cellular Automata", *IEEE 3rd International Symposium on Nanoelectronic and Information Systems (iNIS)*, doi: 10.1109/iNIS.2017.26, (2017).

[3] Soudip Sinha Roy, "Fault tolerance and temperature stability: The dynamic error estimationin quantum dot cellular automata", *IEEE 3rd International Symposium on Nanoelectronic and Information Systems (iNIS)*, doi: 10.1109/iNIS.2017.27, (2017).

[4] Gino A. Dilabio, Edmonton (CA); Robert A. WolkoW, Edmonton (CA); Jason L. Pitters, Edmonton (CA); Paul G. Piva, Edmonton (CA), "Atomistic Quantum Dots", Pub. No. US2015/0060771 A1, 5th May 2015.

[5] Soudip Sinha Roy, "Simplification of master power expression and effective power detection of QCA device (Wave nature tunneling of electron in QCA device)," *2016 IEEE Students' Technology Symposium (TechSym)*, Kharagpur, pp. 272-277, 2016, doi: 10.1109/TechSym.2016.7872695.

[6] Soudip Sinha Roy, "An intelligent mathematical QCA power analysis technique in wave nature of electrons," *2016 6th International Conference - Cloud System and Big Data Engineering (Confluence)*, Noida, pp. 680-684, 2016, doi: 10.1109/CONFLUENCE.2016.7508204.

[7] Chiradeep Mukherjee, Soudip Sinha Roy, Dr. Saradindu Panda, Dr. Bansibadan Majhi, "T- Gate: concept of partial polarization in quantum dot cellular automata", *proc. of IEEE 20th international conf. on VLSI Design and Test (VDAT)*, India, 2016, doi: 10.1109/ISVDAT.2016.8064844.

[8] Yuhui Lu, Mo Liu, and Craig Lent, "Molecular quantum-dot cellular automata: From molecular structure to circuit dynamics", JOURNAL OF APPLIED PHYSICS, 102, 034311, 2007

[9] M. B. Tahoori, Jing Huang, M. Momenzadeh and F. Lombardi, "Testing of quantum cellular automata," in IEEE Transactions on Nanotechnology, vol. 3, no. 4, pp. 432-442, Dec. 2004.

[10] SHIFATUL ISLAM, MOHAMMAD ABDULLAH-AL-SHAFI AND ALI NEWAZ BAHAR, "Implementation of Binary to Gray Code Converters in Quantum Dot Cellular Automata", DOI: 10.15415/jotitt.2015.32010

[11] H. Cho and E. E. Swartzlander Jr., "Adder and Multiplier Design in Quantum-Dot Cellular Automata," in IEEE Transactions on Computers, vol. 58, no. 6, pp. 721-727, June 2009.

[12] Young-Won You, Jun-Cheol Jeon, "Low Complexity QCA Binary to Gray Code Converter", Advanced Science and Technology LettersVol.144 (UBWCN 2017), pp.46-50 DOI: 10.14257/astl.2017.144.06.

[13] Nandini G. Raoa, P.C. Srikantha, Preeta Sharanb, "A novel quantum dot cellular automata for 4-bit code converters", Optik, Elsevier, DOI: 10.1016/j.ijleo.2015.12.119, 2015.

[14] M. G. Waje and P. K. Dakhole, "Design and simulation of new XOR gate and code converters using Quantum Dot Cellular Automata with reduced number of wire crossings," 2014 International Conference on Circuits, Power and Computing Technologies [ICCPCT-2014], Nagercoil, 2014, pp. 1245-1250. doi: 10.1109/ICCPCT.2014.7054942

Soudip Sinha Roy

Author's signature

[15] Mohammad Thaerifard, Mahmmod Fathy, “Improving logic function synthesis through wire crossing reduction in quantum-dot cellular automata layout”, IEEE trans. on Devices and Syatems, IET ciruits, vol. 9, no. 4, pp. 265-274, July 2015.

[16] Soudip Sinha Roy"pGate: An Introduction to A Novel Universal Gate and Power Drop Calculation of QCA circuits" *International Journal Of Engineering And Computer Science (IJECS),* https://www.ijecs.in, Volume 6 Issue 4, 20967-20972, April 2017, DOI: 10.18535/ijecs/v6i4.31.

[17] V. K. Mishra and H. Thapliyal, "Heuristic Based Majority/Minority Logic Synthesis for Emerging Technologies," 2017 30th International Conference on VLSI Design and 2017 16th International Conference on Embedded Systems (VLSID), Hyderabad, 2017, pp. 295-300. doi: 10.1109/VLSID.2017.27.

[18] Mo Liu and C. S. Lent, "Power dissipation in clocked quantum-dot cellular automata circuits," 63rd Device Research Conference Digest, 2005. DRC '05., Santa Barbara, CA, 2005, pp. 123-124. doi: 10.1109/DRC.2005.1553086.

[19] Davoud Bahrepour, "A Novel Full Comparator Design Based on Quantum-Dot Cellular Automata", International Journal of Information and Electronics Engineering, Vol. 5, No. 6, pp. 406-410, November 2015, DOI:10.7763/IJIEE.2015.V5.568.

[20] Robert A. Wolkow, Lucian Livadaru, Jason Pitters, Marco Taucer, Paul Piva, Mark Salomons, Martin Cloutier, Bruno V. C. Martins, "Silicon Atomic Quantum Dots Enable Beyond-CMOS Electronics", Springer Field-Coupled Nanocomputing, pp 33-58, vol. 8280.

[21] Qcadesigner online. Avaliable at http://www.qcadesigner.ca/





Author’s signature